Lamellar Solid-Liquid Mesophase Nucleated by Josephson Vortices at the Melting of the Vortex Lattice in $Bi_2Sr_2CaCu_2O_{8+\delta}$ Superconductor

Y. Segev,[1,†] Y. Myasoedov,[1] E. Zeldov,[1] T. Tamegai,[2] G. P. Mikitik,[3] and E. H. Brandt[4,*]

[1]*Department of Condensed Matter Physics, Weizmann Institute of Science, Rehovot 76100, Israel*
[2]*Department of Applied Physics, The University of Tokyo, Hongo, Bunkyo-ku, Tokyo 113-8656, Japan*
[3]*B. Verkin Institute for Low Temperature Physics & Engineering, National Ukrainian Academy of Sciences, Kharkov 61103, Ukraine*
[4]*Max-Planck-Institut für Metallforschung, D-70506 Stuttgart, Germany*
(Received 2 June 2011; published 9 December 2011)

The local effect of the Josephson vortices on the vortex lattice melting process in $Bi_2Sr_2CaCu_2O_{8+\delta}$ crystals in the presence of an in-plane field H_{ab} is studied by differential magneto-optical imaging. The melting process is found to commence along the Josephson vortex stacks, forming a mesomorphic phase of periodic liquid and solid lamellas, the direction and spacing of which are controlled by H_{ab}. The reduction of the local melting field H_m along the Josephson vortex stacks is more than an order of magnitude larger than the reduction of the average bulk H_m by H_{ab}.

The melting of the vortex lattice in type II superconductors (SCs) [1] is an exemplary phase transition that allows direct imaging of the melting process with control over the interparticle interaction, degree of quenched disorder, and the anisotropy of the host crystal. This phase transition was extensively studied in $Bi_2Sr_2CaCu_2O_{8+\delta}$ (BSCCO), which is a layered high-T_c SC with very high anisotropy $\gamma = \lambda_c/\lambda_{ab} \approx 500$, where λ_c and λ_{ab} are out of plane and in-plane penetration depths. In such layered SCs the energetic cost of penetration of an in-plane field H_{ab} is so low that the SC becomes almost "transparent" to H_{ab}. As a result, the macroscopic magnetic response of the SC, as well as the vortex lattice melting transition $H_m(T)$, are mainly governed by the c-axis field H_c. Experimental and theoretical studies have accordingly shown that in order to appreciably change the melting field H_m in such layered systems, H_{ab} has to be 2–3 orders of magnitude larger than H_c. In BSCCO, in particular, H_m was found to decrease linearly with H_{ab}, $H_m = H_m^0 - \alpha|H_{ab}|$ with $\alpha \sim 0.01$, for not too high H_{ab} [2,3].

In contrast to its very weak average effect, H_{ab} has a major impact on the *local* vortex lattice structure. While H_c results in an hexagonal lattice of two-dimensional pancake vortices (PVs) [4], H_{ab} gives rise to an oblate lattice of Josephson vortex (JV) stacks which may coexist with the PV lattice forming a *crossing lattices* state [3,5] with an attractive interaction between the PVs and JV stacks. As a result, the hexagonal PV lattice is replaced by one of the following configurations, depending on the microscopic parameters and the densities of PVs and JVs [3,6,7]. At low H_c, the *chain state* is obtained in which the PV stacks reside only along the 2D planes formed by the JV stacks (parallel to H_c and H_{ab}), which we refer to as JV planes (JVPs). At high H_c, the JVPs cause only a weak perturbation, resulting in a smooth modulation of the vortex density in the 3D lattice in the direction perpendicular

to the JVPs—*modulated Abrikosov lattice*. The most interesting regime, however, occurs at intermediate values of H_c, in which vortex chains residing on the JVPs coexist with a 3D Abrikosov lattice that occupies the "bulk" between the JVPs forming a *mixed chain and lattice state* as observed by decorations [8], magneto-optics [9,10], scanning Hall probe [11], and Lorentz microscopy [12]. In this mixed regime, Fig. 1(a), a *inhomogeneous* binary system is formed, consisting of two qualitatively different
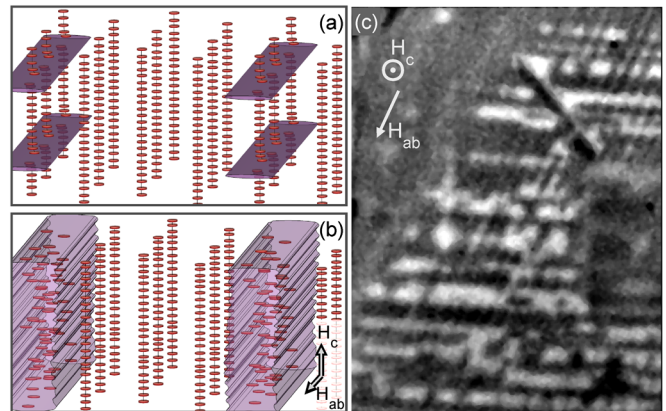
FIG. 1 (color online). (a) Solid crossing lattices state of pancake (red) and Josephson (purple) vortices. PVs residing along the JVs form chain structure whereas PV stacks in-between the JV planes form an Abrikosov lattice. For clarity, the spacing and dimensions of the JVs are shown not to scale. (b) Schematics of lamellar mesophase in which a solid PV lattice coexists with a PV liquid along the JV planes. In the liquid lamellas both the PVs and the JVs may be fully dissociated forming "gas" lamellas. (c) A field-modulated DMO image showing preferential nucleation of melting along the JVs (bright diagonal lines) at $H_c = 15$ Oe, $\delta H = 0.5$ Oe, $H_{ab} = 30$ Oe, $\varphi = 30°$, and $T = 86.5$ K. The characteristic horizontal features are due to sample inhomogeneities. The image is 0.3 mm wide.

subsystems with different dimensionalities, local effective anisotropies, and elastic moduli. So far, the melting transition in presence of H_{ab} was treated only in an effective "homogeneous medium" approach assuming a single bulk $H_m(T)$ [3]. However, since the two vortex subsystems are significantly different, an emerging fundamental question is whether such a binary system, instead of having a single transition, may display two separate transitions—one for each of the subsystems. This would imply a phase separation on the scale of a single vortex lattice unit cell, resulting in an intermediate periodic solid-liquid mesophase with a lamellar structure; see Fig. 1(b).

In this work we address this question experimentally. We find that JVs significantly alter the PV melting landscape resulting in two distinctive melting processes. The JVPs cause a *local* reduction in $H_m(T)$ which is an order of magnitude larger than the average effect of H_{ab}. As a result, a periodic solid-liquid structure is formed similar to lamellar mesophases in liquid crystals, silicates, and various organic compositions [13]. The characteristic feature of these molecular mesophases is their heterogeneous chemical composition. In contrast, the vortex lattice is a unique example of an initially homogeneous system that can be readily driven into a lamellar solid-liquid structure in which the direction, spacing, and thickness of the two types of lamellas can be controlled by tilting the applied magnetic field.

Magneto-optics was previously used for imaging PV-decorated JVs [9,10,14] and vortex lattice melting [14–18]. Here we use differential magneto-optics (DMO) for microscopic imaging of the melting process in the presence of JVs. The data were obtained on an optimally doped BSCCO crystal of $2750 \times 740 \times 30$ μm^3 with $T_c \approx 91$ K and anisotropy $\gamma \approx 500$. Qualitatively similar results were obtained on several other optimally doped samples.

In field-modulated (or temperature-modulated) DMO the difference of two images of the local induction $B(x, y)$ taken at $T_0, H_0 \pm \delta H$ (or $T_0 \pm \delta T, H_0$) is acquired and averaged ~ 10 times. The resulting DMO images visualize the *local* $dB/dH(x, y)$ [or $dB/dT(x, y)$]. Since the first-order melting $H_m(T)$ is accompanied by a steplike discontinuity in B [19] and hence by a peak in dB/dH and dB/dT [20], regions in the sample that are driven through the phase transition by the modulation $2\delta H$ (or $2\delta T$) display in DMO images significantly enhanced dB/dH (or dB/dT) relative to the neighboring regions that remain in the same phase [15]. Figure 2(a) shows a typical field-modulated DMO image of the melting process in BSCCO. The bright broad patches are the regions that undergo melting at $T = 84$ K and $H_c = 24$ Oe within field modulation of 1 Oe. The characteristic long (horizontal) lines are caused by very small compositional inhomogeneities originating from the floating-zone growth process of BSCCO crystals giving rise to small variations in the local
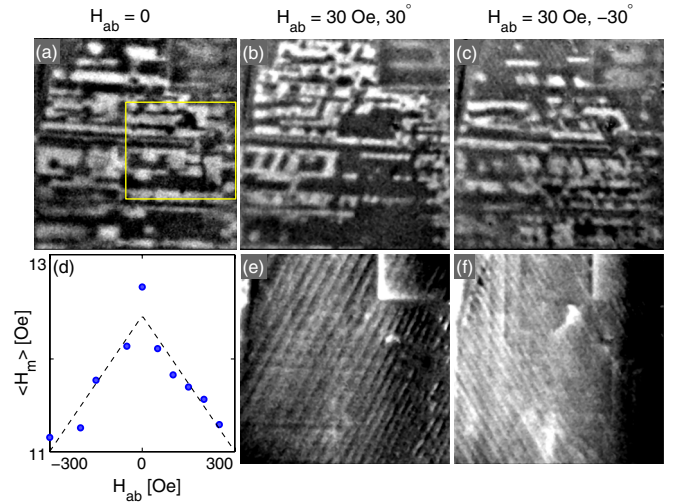

FIG. 2 (color online).　Field-modulated DMO images ($\delta H = 0.5$ Oe) of the melting transition at $T = 84$ K, $H_c = 24$ Oe, $H_{ab} = 0$ (a), $T = 85$ K, $H_c = 20$ Oe, $H_{ab} = 30$ Oe, $\varphi = 30°$ (b), and $T = 85$ K, $H_c = 20.5$ Oe, $H_{ab} = 30$ Oe, $\varphi = -30°$ (c). (e) and (f) DMO images of PV chains at $H_c = 3$ Oe and $H_c = 7$ Oe at the same H_{ab} and T as (b) and (c), respectively. The images are 0.5 mm wide. (d) The average melting field H_m vs H_{ab} at $T = 87$ K (●) and a linear fit $H_m = 12.4$ Oe $- 4 \times 10^{-3}|H_{ab}|$.

$H_m(T)$ as described previously [16]. As shown below, this quenched-disorder-induced landscape is dramatically altered in the presence of H_{ab}.

We first evaluate the *mean* effect of H_{ab} by calculating the average melting field $\langle H_m \rangle$ from a series of DMO images vs H_c at various H_{ab}. Figure 2(d) shows the very weak monotonic decrease of $\langle H_m \rangle$ with H_{ab} that can be described by $\langle H_m \rangle \simeq \langle H_m \rangle_0 - 4 \times 10^{-3}|H_{ab}|$, consistent with previous reports [2,3]. The *local* effect of the JVs on the melting landscape is demonstrated in Figs. 2(b) and 2(c), which show the melting transition for $H_{ab} = 30$ Oe, applied at in-plane angles φ of 30° and $-30°$ relative to the vertical axis of the images. The melting patterns in the presence of H_{ab} are markedly different from Fig. 2(a) having much finer structure and pronounced diagonal orientation along the direction of H_{ab}. For comparison, Figs. 2(e) and 2(f) show DMO images at the same conditions but at lower values of H_c at which the solid chain state is visible as diagonal lines crossing the sample. The comparison of the melting and chain images clearly demonstrates that the JVs have a strong *local* effect on the melting transition rather than just a weak uniform suppression of H_m. They locally alter the mechanism and the effective dimensionality of the melting nucleation and propagation processes inducing periodic structure that has the same spacing and orientation as the JV stacks. Figure 1(c) shows an expanded view of the diagonal melting patterns at a higher temperature and the corresponding full movie of the melting process is available online [21].

The interplay between the sample growth inhomogeneities and the JV lattice is demonstrated in detail in Fig. 3 that shows a magnified view [yellow rectangle in Fig. 2(a)] of the melting transition by sweeping H_c in the presence of a widely spaced JV lattice, $H_{ab} = 5$ Oe, $\varphi = 30°$. The figure shows that melting nucleates first at the crossings points between the JVPs and the horizontal growth inhomogeneities [e.g., along the lower black arrow in Fig. 3(a)]. In Fig. 3(b) the melting expands in-between the JVPs but only within the horizontal defects. In the next step, Fig. 3(c), the melting propagates into the rather uniform wider regions in-between the horizontal defect lines [e.g., the region between the two black arrows in Fig. 3(a)]. Interestingly, within these homogeneous regions the melting starts along the JVP forming periodic structure of liquid lamellas with a period of about 35 μm. The initial apparent thickness of the liquid lamellas is very small $\sim$4 μm, limited by the spatial resolution of our system. With increasing H_c the liquid lamellas expand, Fig. 3(d), followed by melting of the rest of the lattice at still higher H_c.

In order to quantify the effect of the JV lattice on the melting, we perform a very fine scan of H_c with 50 mOe steps and find the melting field $H_m(T, H_{ab}; x, y)$ at each pixel, defined as the first H_c at which the pixel differential intensity reaches a threshold value. Figure 3(e) shows the resulting melting landscape along a narrow strip between the two gray arrows in Fig. 3(a), from which a smoothed, averaged, $\langle H_m \rangle$ has been subtracted for clarity. The modulation of H_m by the JVPs is clearly visible with a modulation amplitude of $\Delta H_m = 0.7 \pm 0.2$ Oe. Note that in order to achieve such ΔH_m shift within the homogeneous

medium approach, one requires $H_{ab} \approx 200$ Oe [see, e.g., Fig. 2(d)], whereas Fig. 3(e) shows such a reduction, locally, with $H_{ab} = 5$ Oe. Thus the *local* modulation of H_m by the JVs is more than an order of magnitude larger than their average effect. A similar analysis was performed on the local behavior of $T_m(H_c, H_{ab}; x, y)$ using a fine temperature scan, where it was found that the JVs induce a modulation $\Delta T_m \simeq 0.1$ K. The two results are consistent taking into account the slope of the melting line $\partial H_m / \partial T_m \approx 5$ Oe/K in optimally doped BSCCO close to T_c [19,22]. Another interesting observation in Fig. 3(e) is the shape of the H_m modulation, which often shows a sharp V-shaped dip at the JVPs and a rather flat maximum between the dips. This implies that the suppression of H_m by the JVPs is very local resulting in formation of liquid lamellas [see Fig. 1(b)] that can be as thin as a "monolayer" of PV stacks which is about 1–2 μm within our experimental conditions and is below our spacial resolution.

Our results can be summarized as follows: (i) JVPs locally suppress $H_m(T)$ of the PV lattice forming a mesomorphic phase of parallel solid-liquid lamellas with a direction and periodicity that are controlled by H_{ab}. (ii) Quenched disorder due to variations in crystal growth conditions introduce large scale variations in local $H_m(T)$ while JVs cause a controllable secondary melting corrugation on a fine scale. (iii) In more disordered regions, vortex liquid droplets are formed at intersection points between the JVs and the growth disorder planes. (iv) The liquid lamellas on the JVPs appear to maintain their alignment even if separated by macroscopic liquid regions.
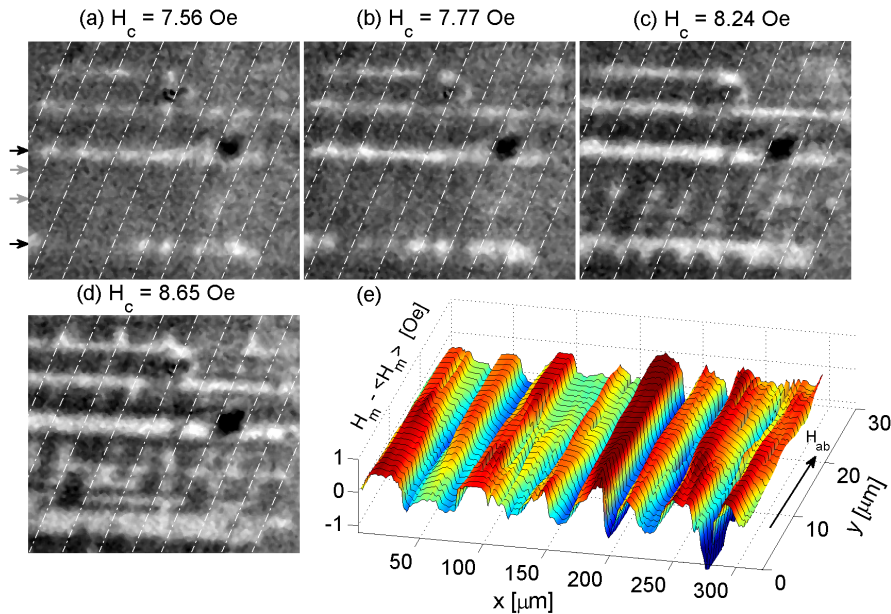

FIG. 3 (color online). (a)–(d) Sequence of temperature-modulated DMO images ($\delta T = 0.2$ K) showing the progression of the melting transition with H_c at $T = 87$ K and $H_{ab} = 5$ Oe, $\varphi = 30°$ in the marked region in Fig. 2(a). The dashed lines are guide to the eye for the location of JVPs. The images are 270 μm wide. (e) The measured variation of the local melting field H_m across the JVPs showing a modulation of 0.7 ± 0.2 Oe.

The melting transition occurs when the induction B_c reaches $B_m(T)$. Since the density of PVs and hence B_c along the JVPs is higher than in-between them, one may argue that the observed melting along the JVs is a result of the enhancement of the local B_c by ~ 0.7 G, rather than JV-induced suppression of the local B_m. We find that the enhancement of B_c on the JV stacks is large only close to the penetration field [10] as seen in Figs. 2(e) and 2(f). Upon increasing H_c, the DMO visibility of the JV stacks decreases monotonically and vanishes well below H_m, whereas a 0.7 G spatial modulation in B_c should have been well within our experimental resolution even in non-differential images. We therefore, conclude that the dominant mechanism of formation of the lamellar structure is the modulation of the local B_m by the JV lattice.

A priori, it is not obvious that the melting should nucleate on the JV stacks. The stiff binding potential of the JVP might suppress thermal fluctuations of the PV chain and hence shift H_m to higher fields, similar to the H_m enhancement found in BSCCO in the presence of a low concentration of columnar defects [17]. On the other hand, Lorentz microscopy has shown that in very thin BSCCO, the PV vibrations along the chains are significantly enhanced due to incommensurability between the chain and the adjacent lattice [12], which can explain the experimental observation of a reduction of $H_m(T)$ on the chains.

The magnitude of the local reduction of H_m on the JVPs can be roughly compared with the global measurements as follows. In global measurements the separate melting transitions of the chains and the lattices will be observable as single broadened transition. Assuming that the JVs suppress the melting only within their core region $\lambda_{J0} = \gamma s \approx 0.75$ μm (s is the interlayer spacing), we can evaluate the global ΔH_m as a volume weighted average of the local transitions. In Fig. 3, at $H_{ab} = 5$ Oe, the local melting suppression on the JVPs is $\Delta H_m = 0.7$ Oe, and the average distance between the JVPs is $a_J = 36$ μm, resulting in a weighted global $\Delta H_m = (\lambda_{J0}/a_J) \times 0.7$ Oe $= 1.5 \times 10^{-2}$ Oe. Assuming a linear H_{ab} dependence we obtain $\alpha = \Delta H_m/H_{ab} = 3 \times 10^{-3}$, which is in a general agreement with published results [2,3] and Fig. 2(d).

In our experimental range of $B_c \lesssim 45$ G the intervortex spacing is larger than the JV core, $a_0 > \lambda_{J0}$, so that each JVP is occupied by a single row of PVs. This fact, combined with the observation that the melting nucleates along the JVPs, suggests that at the onset of melting liquid "vortex monolayer" lamellas are formed along the JVPs that are "sandwiched" between thicker lamellas of vortex solid. This may present a very interesting case of interacting vortex lines in a '1 + 1'-dimensional random potential or of a Luttinger liquid [23,24]. The properties of such a liquid monolayer of lines is unclear, in particular, taking into account the incommensurate periodic potential induced by the two adjacent solids. Moreover, the first-order melting in BSCCO is believed to be a "sublimation"

transition—simultaneous melting and layer decoupling—resulting in a PV "gas" with no c-axis correlations [3,25]. This constitutes an even more intriguing situation in which "gas" lamellas are caged between solid lamellas. Remarkably, in such a mesostate the JVs may cease to exist due to the random motion of the PVs along the "gas" lamellas resulting in Josephson "sheets", where the CuO_2 planes are fully decoupled in the "gas" monolayers and fully coupled in the solid regions. This situation is schematically depicted in Fig. 1(b).

Our finding of the heterogeneous behavior questions the validity of existing approaches in which H_{ab} is considered as a source of a uniform $H_m(T)$ reduction in an effective homogeneous medium [3]. In particular, if one assumes that the suppression of the local $H_m(T)$ is related to the local density of JVs or of the crossing points between the JVs and the PV stacks, one may expect $\Delta H_m \propto \sqrt{H_{ab}}$ along the JVPs and $\Delta H_m = 0$ in-between them. Since the density of the JVPs also grows as $\sqrt{H_{ab}}$, this should result in an average $\Delta H_m \propto H_{ab}$ as observed by the global measurements. Another important question that our findings raise is the stability of mesophase. On one hand the liquid lamellas destroy the shear modulus and may act as a source of dislocations that destabilize the solid lamellas, reducing their H_m. On the other hand, a finite solid-liquid surface tension [15] may stabilize the solid lattice against formation of liquid lamellas.

In summary, we have shown that in contrast to its very weak average influence, the crossing JV lattice has a major effect on the *local* melting process of the vortex lattice in BSCCO. At low in-plane fields, the JV stacks reduce the local melting field of the PV lattice by about 0.7 Oe. As a result, within homogeneous regions of the sample, melting is nucleated along the plains containing the JV stacks forming a periodic lamellar solid-liquid or solid-"gas" mesophase with periodicity and direction that are controlled by the in-plane field. We suggest that the PV liquid or "gas" lamellas can be as thin as a PV "monolayer". These findings raise a number of intriguing theoretical and experimental questions including the microscopic origin of the liquid nucleation along the JVs, the properties of the 2D lamellas of vortex liquid or "gas", and the possible destruction of the JV lattice in the lamellar mesostate.

---

*Deceased.
†yehonathan.segev@gmail.com

[1] G. Blatter *et al.*, Rev. Mod. Phys. **66**, 1125 (1994); G. P. Mikitik and E. H. Brandt, Phys. Rev. B **64**, 184514 (2001).

[2] B. Schmidt *et al.*, Phys. Rev. B **55**, R8705 (1997); S. Ooi *et al.*, Phys. Rev. Lett. **82**, 4308 (1999); J. Mirković *et al.*, *ibid.* **86**, 886 (2001).

[3] A. E. Koshelev, Phys. Rev. Lett. **83**, 187 (1999).

[4] J. R. Clem, Phys. Rev. B **43**, 7837 (1991).

[5] S. J. Bending and M. J. W. Dodgson, J. Phys. Condens. Matter **17**, R955 (2005).

[6] L. N. Bulaevskii, M. Ledvij, and V. G. Kogan, Phys. Rev. B **46**, 366 (1992).

[7] A. E. Koshelev, Phys. Rev. B **71**, 174507 (2005).

[8] C. A. Bolle *et al.*, Phys. Rev. Lett. **66**, 112 (1991); I. V. Grigorieva *et al.*, Phys. Rev. B **51**, 3765 (1995); M. Tokunaga *et al.*, *ibid.* **67**, 134501 (2003).

[9] V. K. Vlasko-Vlasov *et al.*, Phys. Rev. B **66**, 014523 (2002); M. Tokunaga *et al.*, *ibid.* **66**, 060507 (2002).

[10] Y. Segev *et al.*, Phys. Rev. B **83**, 104520 (2011).

[11] A. Grigorenko *et al.*, Nature (London) **414**, 728 (2001); A. N. Grigorenko *et al.*, Phys. Rev. Lett. **89**, 217003 (2002).

[12] T. Matsuda *et al.*, Science **294**, 2136 (2001).

[13] A. Monnier *et al.*, Science **261**, 1299 (1993); J.-C. P. Gabriel *et al.*, Nature (London) **413**, 504 (2001).

[14] M. Yasugaki *et al.*, Phys. Rev. B **65**, 212502 (2002).

[15] A. Soibel *et al.*, Nature (London) **406**, 282 (2000).

[16] A. Soibel *et al.*, Phys. Rev. Lett. **87**, 167001 (2001); M. Yasugaki *et al.*, Phys. Rev. B **67**, 104504 (2003).

[17] S. S. Banerjee *et al.*, Phys. Rev. Lett. **93**, 097002 (2004).

[18] S. Goldberg *et al.*, Phys. Rev. B **79**, 064523 (2009).

[19] E. Zeldov *et al.*, Nature (London) **375**, 373 (1995).

[20] N. Morozov *et al.*, Phys. Rev. B **54**, R3784 (1996).

[21] See Supplemental Material at http://link.aps.org/supplemental/10.1103/PhysRevLett.107.247001 for movies of the melting process.

[22] H. Beidenkopf *et al.*, Phys. Rev. Lett. **98**, 167004 (2007).

[23] C. A. Bolle *et al.*, Nature (London) **399**, 43 (1999).

[24] T. Nattermann, T. Giamarchi, and P. Le Doussal, Phys. Rev. Lett. **91**, 056603 (2003).

[25] G. Blatter *et al.*, Phys. Rev. B **54**, 72 (1996); D. T. Fuchs *et al.*, *ibid.* **55**, R6156 (1997); B. Horovitz and T. R. Goldin, Phys. Rev. Lett. **80**, 1734 (1998); T. Shibauchi *et al.*, *ibid.* **83**, 1010 (1999).